Ethylene Vinyl Acetate - Cloisite Nanocomposite Membranes and their Gas Separation Behavior

A. R. Ramadan[*], A.M.K. Esawi[**], A. Abdel-Hafiz[***],
C. Charmette [****] and A. Ayral[*****]

[*]Yousef Jameel Science and Technology Center, The American University in Cairo, AUC Avenue, New Cairo 11835, Egypt, aramadan@aucegypt.edu
[**]Yousef Jameel Science and Technology Center, The American University in Cairo, AUC Avenue, New Cairo 11835, Egypt, a_esawi@aucegypt.edu
[***]Yousef Jameel Science and Technology Center, The American University in Cairo, AUC Avenue, New Cairo 11835, Egypt, ali.ahmad@aucegypt.edu
[****]IEM, CC047, Université Montpellier 2, Place Eugène Bataillon, 34095 Montpellier, France, christophe.charmette@univ-montp2.fr
[*****]IEM, CC047, Université Montpellier 2, Place Eugène Bataillon, 34095 Montpellier, France, andre.ayral@univ-montp2.fr

ABSTRACT

Nanocomposite membranes of Ethylene Vinyl Acetate (EVA) with Cloisite 20A and 30B montmorillonite clays were prepared by a novel combination of solution compounding, extrusion and compression molding in order to achieve a good dispersion of the clay within EVA. X-ray diffraction and TEM analysis showed that the EVA-C20A nanocomposite primarily contained intercalated clay structures, whereas the EVA-C30B primarily contained exfoliated clay structures. This difference was found to lead to different gas permeability and selectivity behaviors.

Keywords: membranes, ethylene vinyl acetate, montmorillonite clay, gas separation

1 INTRODUCTION

Membranes are expected to play a future central role in gas separation. Novel polymer-clay nanocomposite membranes with improved properties and performance have gained recent attention in this regard [1,2]. Ethylene vinyl acetate (EVA) membranes have shown good potential for gas separation, however limited data are available for EVA-clay nanocomposite membranes [3,4]. The difficulty in dispersing and exfoliating the clay in EVA has been the main constraint. The current work aims at understanding the correlation between EVA-montmorillonite (MMT) clay nanocomposite membrane morphology and gas permeation properties.

2 EXPERIMENTAL

A dilute solution of EVA (Sigma Aldrich, 18wt% vinyl acetate) in tetrahydrofuran, THF (Sigma Aldrich, HPLC grade) was prepared. Cloisite-20A and 30B MMT organoclays (Southern Clays Products), pre-dispersed in THF, were then added to this solution and the mixture sonicated at 50 MHz frequency for 30 minutes at 50°C. The amounts of the added clays were such that the final composite contained 5 wt% of MMT. In order to achieve a good dispersion of the clays within EVA, the resulting composites were extruded in a twin screw extruder (XTS 19, Xtrutech) having intermeshing co-rotating screws, with a diameter of 19 mm and L/D = 25. The screws speed was kept constant at 280 r.p.m. and a residence time of 10 min was used. The composites were extruded from a die having three horizontal circular orifices of 1.5 mm diameter. The extrudates were then compression-molded at 140°C and 20 MPa into membranes of 47 mm diameter and approximately 0.5-0.6 mm thickness. This resulted in samples EVA-C20A and EVA-C30B.

Clay	Organic modifier	Modifier amount (wt%)	Interlayer space (nm)
20A	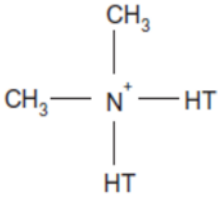	38	2.42
30B	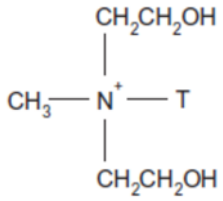	28	1.85

Table 1: MMT clays specifications.

Sample characterization was carried out by a D8 Bruker x-ray powder diffractometer (XRD) operated at 40 kV and 30 mA using at Kα of 0.1542 nm. Transmission electron microscopy (TEM) images were taken by a JEOL 2010 equipment, with a LaB6 electron gun, and operated between 80 and 200kV. Permeation experiments were carried out by using the constant volume and variable pressure technique in a permeability apparatus at 298 K. The apparatus consists essentially of a two-compartment permeation cell separated by the tested membrane. Permeation of He, N_2, CH_4, CO_2 gases was obtained measuring the pressure increase in the downstream compartment (with a constant volume of $3.00x10^{-5}$ m^3) and using different MKS Baratron pressure transducers (range from 0.0 to $1x10^5$ Pa). The films and downstream cell walls where outgased in situ during 24 h at high vacuum using a turbomolecular pump (Leybold, Turbovac 50, 50 $l.s^{-1}$). For calulations of the permeability coefficient, we used the mathematical treatment for thin films based on Fick's second law and reported by Crank [5].

3 RESULTS

3.1 XRD

XRD results indicated that sample EVA-C20A primarily contained intercalated clay structures, as evidenced by the downshift to lower 2-theta of the basal d value of the interlayer space as compared to pristine Cloisite 20A, Figure 1.

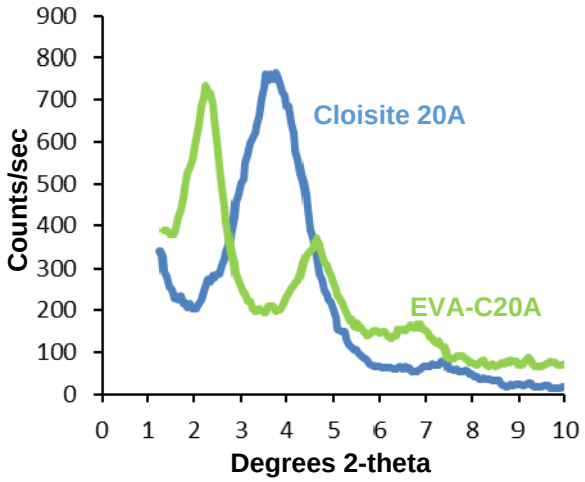

Figure 1: XRD results for pristine Cloisite 20A and sample EVA-C20A.

Sample EVA-C30B, on the other hand, primarily contained exfoliated clay structures, as evidenced by the decrease in the intensity of the basal reflection and its broadening, indicating a delamination of the clay layers, compared to pristine Cloisite 30B, Figure 2.

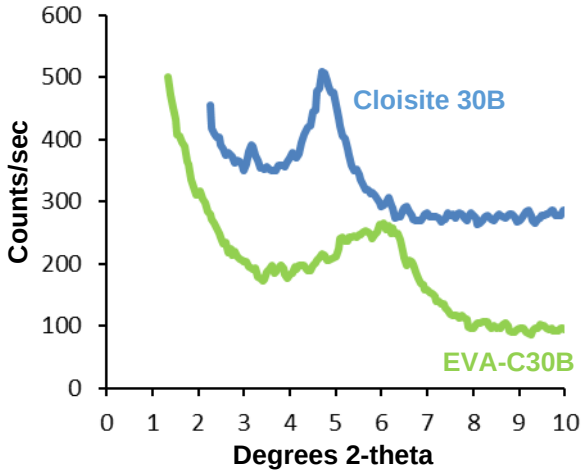

Figure 2: XRD results for pristine Cloisite 30B and sample EVA-C30B.

3.2 TEM

TEM images corroborate XRD results. EVA-C20A exhibited clay stacks with interlayer distance values in agreement with those of the XRD pattern, denoting intercalated structures, Figure 3. These structures are relatively well dispersed in the EVA matrix, though some areas of the polymer were found devoid of clay structures. EVA-C30B on the other hand revealed both stacks of clay layers as well as more numerous individual layers, Figure 4. This supported the XRD results of a more exfoliated clay structure.

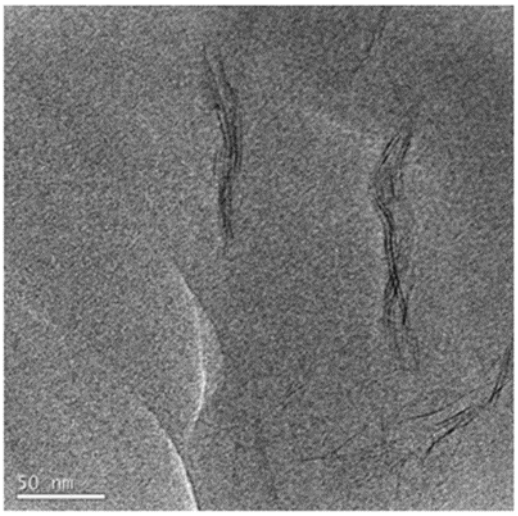

Figure 3: TEM of EVA-C20A displaying intercalated clay layers.

.

	Thickness (μm)	Permeability (Barrer)				Ideal Selectivity		
		He	N_2	CO_2	CH_4	CO_2/He	CO_2/N_2	CH_4/CO_2
EVA	575	6.3	4.8	8.6	11.9	1.4	1.8	1.4
EVA-C20A	640	7.3	7.6	16.3	19.5	2.3	2.2	1.2
EVA-C30B	540	4.2	6.3	1.7	4.3	0.5	0.3	2.2

Table 2: Permeability and selectivity data for different EVA membranes (1 Barrer = 10^{-10} cm^3 (STP).cm/cm^2 .s.cm_{Hg})

Figure 4: TEM of EVA-C30B displaying primarily exfoliated clay layers

The difference in clay behavior within the EVA matrix can be related to the higher compatibility between the organic modifier of Cloisite 30B and EVA. It is believed that the organic modifier in Cloisite 30B which contains an (OH) group has facilitated the dispersion and delamination of clay layers, as it favors interaction with the acetate polar sided group in EVA.

3.3 Gas permeability and selectivity

Results indicated that permeability and selectivity varied with the type of organoclay present in the matrix. EVA-C20A membranes exhibited the highest gas permeability, while EVA-C30B membranes exhibited the lowest (except for N_2).

As noted earlier, XRD and TEM results indicated that the EVA-C20A membranes primarily contained well-dispersed intercalated clay structures, whereas EVA-C30B membranes mostly contained well-dispersed exfoliated clay structures. The differences in gas permeability could be explained in terms of these observations. For EVA-C20A, the lower compatibility between EVA chains and Cloisite-20A organic modifier would lead to the perturbation of polymer chain packing as a result of the presence of the clay filler, with possible nanoscale gaps between clay particles and polymer matrix, and gas diffusion through the polymer-clay interface and the clay interlayer space [2]. On the other hand, an increase of tortuosity because of the exfoliated structure as well as the better compatibility between EVA chains and Cloisite-30B organic modifier, would lead to an increased polymer packing with minimal gaps between clay particles and polymer matrix with limited gas diffusion.

As for selectivity results, EVA-C20A membranes generally exhibited slightly enhanced gas separation over neat EVA. In parallel with a decrease of the permeability of CO_2 for EVA-C30, this membrane showed lower selectivity values relative to neat EVA with the exception of CH_4/CO_2 mixture. These preliminary results should be later completed with additional experiments on nanocomposite membranes containing different weight percentages of clays and by studying the variation of both permeability and ideal selectivity versus temperature. It should help us to de-correlate the contributions of the EVA matrix, of the exfoliated clays and of the organic modifier to the gas transport across these membranes.

4 CONCLUSION

A novel combination of solution compounding, extrusion and compression molding was used to prepare EVA-Cloisite MMT nanocomposites. It was successful in achieving a good dispersion of the clays within EVA. The clay structure in the nanocomposite was found to depend on the organic modifier present. For Cloisite 20A, where the organic modifier is of limited compatibility with EVA, intercalated structures were mostly obtained. On the other hand, Cloisite 30B led to exfoliated structures as a result of the better compatibility between its organic modifier and EVA.

The nanocomposite structure was found to affect the gas permeability and gas selectivity properties of the samples, with EVA-Cloisite 20A exhibiting higher gas permeability.

REFERENCES

[1] S.A. Hashemifard, A.F. Ismail, T. Matsuura, Chemical Engineering Journal, 170, 316–325, 2011.

[2] A.K. Zulhairun, A.F. Ismail, T. Matsuura, A.S. Abdullah, A. Mustafa, Chemical Engineering Journal, 241, 495-503, 2014.

[3] S. A. Mousavi, M. Sadeghi, M.M.Y. Motamed-Hashemi, M.P. Chenar, R, Roosta-Azad, M. Sadeghi, Separation and Purification Technology, 62, 642–647, 2008.

[4] S.A. Kumar, Y.L. He, Y.M. Ding, Y. Le, M.G. Kumaran, S. Thomas, Industrial and Engineering Chemistry Research, 47, 4898–4904, 2008.
[5] J. Crank, The Mathematics of Diffusion, 2nd Edition, Clarendon, Oxford, 1975.